JOURNAL OF PROPULSION AND POWER
Vol. 25, No. 2, March–April 2009

Experimental Evaluation of Low Pressure-Swirl Atomizer Applied Engineering Design Procedure

Heraldo da Silva Couto*
Center for Technology in Energy, 12247-004 São José dos Campos, SP, Brazil
Pedro Teixeira Lacava†
Aeronautical Technology Institute, 12345-678 São José dos Campos, SP, Brazil
Demetrio Bastos-Netto‡
Center for Technology in Energy, 12247-004 São José dos Campos, SP, Brazil
and
Amílcar Porto Pimenta§
Aeronautical Technology Institute, 12345-678 São José dos Campos, SP, Brazil

DOI: 10.2514/1.37018

In a pressure-swirl atomizer a swirling motion is imparted to the fuel leading it, under the action of centrifugal forces, to spread out in the shape of a hollow cone as soon as it leaves the exit orifice. This kind of atomizer is used in gas turbines and liquid-propellant rockets. The need to minimize the combustor length usually leads to spray angles around 90 deg. The present work presents a procedure to design and verify the experimental behavior for low pressure-swirl atomizers. This atomization condition is especially important, for example, in the case of gas turbine operation under idle regime. The Sauter mean diameter and the spray-cone angle are evaluated and made to fit the calculated atomizer dimensions. The Sauter mean diameter is obtained through the use of a model originally developed for fan-spray atomizers and extended for pressure-swirl atomizers. A pressure-swirl atomizer was manufactured following this design procedure. The discharge coefficient, the spray-cone angle, and the Sauter mean diameter were evaluated experimentally and compared with the theory used to design the atomizer displaying a good matching. The spray Sauter mean diameter was measured with a laser scattering system.

Nomenclature

A_a	=	air core area, m^2
A_p	=	tangential entry passage cross-sectional area, m^2
A_0	=	nozzle orifice exit area, m^2
Cd	=	discharge coefficient
D_L	=	ligament diameter, m
D_p	=	tangential entry passage diameter, m
D_s	=	swirl chamber diameter, m
D_0	=	nozzle discharge diameter, m
FN	=	flow number, nondimensional
h_0	=	liquid sheet thickness at the nozzle tip, m
K	=	atomizer constant, nondimensional
L_p	=	tangential entry passage length, m
L_s	=	swirl chamber length, m
L_0	=	nozzle length, m
$\dot{m}_L$	=	liquid mass flow rate, $kg \cdot s^{-1}$
SMD	=	Sauter mean diameter, m
U_0	=	velocity of the liquid at the atomizer tip, $cm \cdot s^{-1}$
X	=	the ratio between the air core area (A_a) and the nozzle orifice exit area (A_0), nondimensional
ΔP_L	=	injector pressure differential, Pa
θ	=	cone semi-angle, deg
μ_L	=	liquid dynamic viscosity, cp
ρ_a	=	air density, $kg \cdot m^{-3}$
ρ_L	=	liquid density, $kg \cdot m^{-3}$
σ	=	liquid surface tension, $dyne \cdot cm^{-1}$

Received 7 February 2008; revision received 22 August 2008; accepted for publication 1 September 2008.

*Thermal Energy Manager; heraldo.couto@vsesa.com.br.
†Professor, Department of Aeronautical Engineering; placava@ita.br.
‡Chief Scientist; demetrio.bastos@vsesa.com.br. Associate Fellow AIAA.
§Professor, Department of Aeronautical Engineering; amilcar@ita.br.

I. Introduction

THE liquid fuel injection process plays an important role in many aspects of combustion performance. To achieve the surface to mass high ratios in the liquid phase leading to the desired very high rates of evaporation, the liquid fuel must be fully atomized before its arrival at the combustion zone.

Atomization can be accomplished by spreading the fuel into a thin sheet whose induced instability promotes its disintegration into ligaments which then collapse into droplets due to surface tension action. This also can be achieved by discharging the fuel through orifices with specially shaped passages, which also leads it to become a thin sheet from which ligaments and ultimately droplets are formed so that these resulting droplets will be distributed through the combustion zone in a controlled pattern and direction.

In applications where combustion rates must be high, such as, for example, in aircraft gas turbines (around $500,000\ kJ/m^3 \cdot s$), the spray angle must be large, around 90 deg, due to the need of minimizing the combustor length. This can be achieved by imparting a swirling motion to the emerging fuel jet. Much wider cone angles can be obtained using pressure-swirl atomizers where a swirling motion is imparted to the fuel under the action of centrifugal force, spreading it out in the form of a hollow cone upon leaving the exit orifice.

Figure 1 shows schematically a pressure-swirl atomizer. The liquid is fed to the injector through tangential passages giving it a high angular velocity, and forming, in the swirling chamber, a liquid layer with a free internal surface, thus creating a gas-core vortex. The liquid is then discharged from the nozzle in the form of a hollow conical sheet which breaks up into small droplets. In practice, some pressure-swirl atomizers achieve the desired swirling motion by pushing the liquid flow through specially designed helical channels.

As pressure-swirl atomizers play an important role in gas turbine and liquid-propellant rocket engine combustion processes, there are several theoretical and experimental results available on this kind of atomization technique. Lefebvre [1] has organized the most

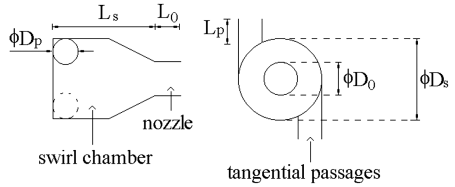

Fig. 1 Pressure-swirl atomizer.

important references on atomization and sprays, including some aspects of pressure-swirl atomizer design procedures, also presenting some predictions on discharge coefficients, spray-cone angles, and mean droplet sizes. The work of Couto et al. [2] suggested a theoretical formulation for estimating the Sauter mean diameter (SMD) of droplets generated by pressure-swirl atomizers. This was done extending the model of Dombrowski and Johns [3] on the disintegration of viscous liquid sheets generated by fan-spray atomizers, the results comparing satisfactorily with available experimental data and other existing empirical models. Jones [4] presented a design optimization of a large pressure-jet atomizer for furnace power plants. Lefebvre [5] discussed the application of pressure-swirl atomizers in gas turbine combustion chambers. Marchione et al. [6] revealed an important result concerning the fluctuating behavior of the spray. Reddy and Mishra [7] experimentally investigated the spray behavior of a pressure-swirl atomizer at low pressure operation. Santolaya et al. [8] performed experimental studies of near-field flow structures in hollow-cone pressure-swirl sprays and observed that when the perforated sheet changed into a wavy-sheet disintegration mode, a notably finer spray with a higher radial dispersion was obtained. The entrained airflow rate showed a significant increase with higher axial velocities at the central zone. The air entrainment process notably affected the droplet mean velocity profiles. In the work of Kim et al. [9], the measurements of breakup length under high ambient pressure showed that the aerodynamic force significantly affects the breakup of the swirling liquid sheets. The breakup length decreased with increasing aerodynamic force as the ambient gas density and Weber number increased.

Paula Souza [10] presented a design procedure and performed an experimental analysis of a coaxial pressure-swirl bipropellant atomizer for liquid-propellant rocket engines. Bazarov and Yang [11] have discussed the liquid-propellant rocket engine pressure-swirl atomizer dynamics and its relation with flow oscillations. Kim et al. [12] observed the influence of recess length in the spray angle and the breakup length for liquid-liquid coaxial swirl injectors. They observed that the variation of the recess length resulted in three different injection regimes: external, tip, and internal mixing injection. In the work of Ramezani and Ghafourian [13] a theoretical model based on momentum balance was developed to predict the combined spray behavior liquid–liquid swirl coaxial injector. The spray angles for different operating conditions were obtained from analysis of high resolution digital images. The experimental observations indicate that the inner and outer sprays are pulled together and interact to form a combined spray. This interaction results in an overall performance which is different from the summation of each individual spray characteristic.

This work describes a procedure for designing a pressure-swirl atomizer to operate under low injector pressure differential conditions. This atomization situation is typical of low power gas turbine operation. The fuel consumption in aircraft gas turbines can change drastically from low power to high power conditions, as, for example, from 1 to 40, while going from ground-idle to takeoff mode. Therefore, some injection systems are able to provide good atomization for both situations, that is, low and high fuel consumption conditions are always needed. In practice, the solution is the use of a dual-orifice atomizer which essentially is composed of two pressure-swirl nozzles concentrically fitted, one inside the other. The pilot nozzle is assembled in the inner position. At low fuel flow rates all the fuel is supplied through the pilot nozzle. However, when the pressure level reaches a predetermined value, the pressurizing valve opens and admits fuel to the main nozzle, which has a high flow number. In spite of the use of dual injection systems, the International Civil Aviation Organization often reports that higher emissions of carbon monoxide and unburned hydrocarbons are observed during low power operations, especially under ground-idle and landing modes. One of the reasons for this behavior is the poor atomization as a consequence of the low pressure injection process.

The SMD and the spray-cone angle are evaluated with the proper atomizer dimensions. The SMD is estimated using the formulation of Dombrowski and Johns [3], extended by Couto et al. [2] for pressure-swirl atomizers, as mentioned above. An atomizer was manufactured based on the suggested design procedure, and its discharge coefficient, spray angle, and SMD were measured and compared with the theoretical estimates of those parameters.

A single injector was manufactured for the experiments, as this work intends to observe the spray characteristics in low pressure injection situations, and not its geometric parameters influence. The effect of these parameters on pressure-swirl atomizer performance is quite well reported, as mentioned in the work of Xue et al. [14]. Therefore, in the present case the injector performed experimentally was designed for typical dimensions, mass flow rates, and injection pressures of gas turbine pilot nozzle in low power operation regimes.

II. Design Considerations and Spray Predictions

The following data are required for an atomizer design: the liquid properties (density, surface tension, and viscosity), the discharging ambient characteristics (ambient pressure and density), and the liquid injection conditions (i.e., the mass flow rate and the injector pressure differential).

First, the flow number, FN, is calculated using Eq. (1):

$$FN = \frac{\dot{m}_L}{\sqrt{\rho_L \cdot \Delta P_L}} \tag{1}$$

where $\dot{m}_L$ is the liquid mass flow rate, ρ_L is the liquid density, and ΔP_L is the injector pressure differential.

The nozzle discharge diameter (D_0) (see Fig. 1) must be chosen and the other remaining atomizer geometrical parameters are obtained considering the following dimensionless groups: $A_P/(D_S \cdot D_0)$, D_S/D_0, L_S/D_S, L_0/D_0, and L_P/D_P, where A_p is the tangential entry passage cross-sectional area. Other important geometrical parameters are also shown in Fig. 1.

The ratio L_S/D_S should be reduced to minimize wall friction losses. However, a limiting value is needed to achieve the liquid flow stabilization and the generation of a uniform vortex sheet. This ratio must be higher than 0.5, and a typical value recommended for proper design is 1.0, as pointed out by Elkobt et al. [15]. The parameter L_0/D_0 should also be reduced to minimize friction losses at the atomizer exit. Further, the ratio L_p/D_p should not be smaller than 1.3 because a short tangential inlet passage channel may generate a diffuse discharge leading to an unstable spray (Tipler and Wilson [16]). Finally, one has to watch out for the obvious limitations of the manufacturing process itself.

The other two dimensionless groups, that is, $A_p/(D_s \cdot D_0)$ and D_s/D_0 both have a considerable influence in the discharge coefficient, which can be calculated by Eq. (2):

$$Cd = \frac{\dot{m}_L}{A_0 \cdot \sqrt{2 \cdot \rho_L \cdot \Delta P_L}} \tag{2}$$

The ratios $A_p/(D_s \cdot D_0)$ and D_s/D_0 can be obtained from empirical relations for Cd developed by Carlisle [17], Risk and Lefebvre [18], and Jones [4], as shown in Eqs. (3–5), respectively:

$$Cd = \left(0.0616 \frac{D_s}{D_0} \cdot \frac{A_p}{D_s \cdot D_0}\right) \tag{3}$$

$$Cd = 0.35 \cdot \left(\frac{D_s}{D_0}\right)^{0.5} \cdot \left(\frac{A_p}{D_s \cdot D_0}\right)^{0.25} \tag{4}$$

$$Cd = 0.45 \cdot \left(\frac{D_0 \cdot \rho_L \cdot U_0}{\mu_L}\right)^{-0.02} \cdot \left(\frac{L_0}{D_0}\right)^{-0.03} \cdot \left(\frac{L_s}{D_s}\right)^{0.05} \cdot \left(\frac{A_p}{D_s \cdot D_0}\right)^{0.52} \cdot \left(\frac{D_s}{D_0}\right)^{0.23} \tag{5}$$

In fact, the Cd calculated using the flow parameters in Eq. (2) can be used to choose appropriate values for $A_p/(D_s \cdot D_0)$ and D_s/D_0 using Carlisle results [Eq. (3)], so that Cd is recovered with the Risk and Lefebvre and Jones equations [i.e, with Eqs. (4) and (5), respectively] to check for discrepancies. Nevertheless, intervals ranging from 0.19 to 1.21 and from 1.41 to 8.13 are recommended for $A_p/(D_s \cdot D_0)$ and D_s/D_0, respectively [1]]. Jeng et al. [19] have conducted a computational and experimental study of the influence of $A_p/(D_s \cdot D_0)$ on the spray angle, being found that an increase in this ratio results in decreasing the spray angle and increasing the liquid film thickness in large scale nozzles. Additionally, the results of Jeng et al. [19] have shown that theoretical correlations based on inviscid flow assumptions underestimate the film thickness, and overestimate the spray angle significantly. In the case of D_s/D_0, Sakman et al. [20] have shown that an increase in D_s/D_0 results in a decrease in the film thickness, in the discharge coefficient, and in the spray angle.

Equation (5) reported by Jones [4], is the most elaborate one, showing that the ratios $A_p/(Ds \cdot D_0)$ and Ds/D_0 are the dominant dimensionless parameters in the calculation of Cd.

In the present design procedure, the critical atomizer dimensions can be accepted or not, depending on the calculated values of the spray half angle (θ) and the mean drop diameter.

The semi-angle (θ) can be estimated by the expression developed by Giffen and Muraszew [21] for a pressure-swirl atomizer (under ideal conditions):

$$\sin\theta = \frac{(\pi/2) \cdot Cd}{K \cdot (1 + \sqrt{X})} \tag{6}$$

where $K = A_P(D_S \cdot D_0)$ (the atomizer constant) and X is the ratio between the air core area (A_a) and the nozzle orifice exit area (A_0), obtained by Eq. (7):

$$D_0 = 2 \cdot \sqrt{\frac{FN}{\pi \cdot (1 - X) \cdot \sqrt{2}}} \tag{7}$$

With the FN and the spray-cone semi-angle (θ), obtained from Eqs. (1) and (6), respectively, it is possible to estimate the liquid sheet thickness at the nozzle tip, h_0, as suggested by Couto et al. [2]:

$$h_0 = \frac{0.00805 \cdot FN \cdot \sqrt{\rho_L}}{D_0 \cdot \cos\theta} \qquad (\mathrm{m} \cdot \mathrm{kg} \cdot \mathrm{s}\ \text{units}) \tag{8}$$

Dombrowski and Johns [3] derived an expression for estimating the ligament diameter D_L, formed on the liquid film breakup of a thin plane sheet as the one generated by a fan-spray atomizer. Couto et al. [2] extended this result for a pressure-swirl atomizer. They assumed that the conical sheet possesses a rupture radius much larger than its thickness so that once the conical sheet is established the amplitude of any disturbance (ripple) away from the injector tip is much smaller than the cone diameter (so that the ripple "sees" the conical sheet as a plane sheet). Couto et al. also assumed that the wavelength of any ripples formed in the liquid film until its amplitude is equal to the ligament radius, so that one droplet is produced per wavelength. The ligament diameter is given by

$$D_L = 0.9615 \cdot \cos\theta \cdot \left(\frac{h_0^4 \cdot \sigma^2}{U_0^4 \cdot \rho_a \rho_L}\right)^{1/6} \cdot \left[1 + 2.6 \cdot \mu_L \cdot \cos\theta \left(\frac{h_0^2 \cdot \rho_a^4 \cdot U_0^7}{72 \cdot \rho_L^2 \cdot \sigma^5}\right)^{1/3}\right]^{0.2} \tag{9}$$

where σ (dyne/cm) is the liquid surface tension, ρ_a (g/cm^3) is the air density of the surrounding medium, μ_L (cp) is the liquid dynamic viscosity, and U_0 (cm/s) is the velocity of the liquid at the atomizer tip, given by Eq. (11):

$$U_0 = \sqrt{\frac{2\Delta P_L Cd}{\rho_L}} \tag{10}$$

$$h_0 = \frac{D_0 - [D_0^2 - (4\dot{m}/\pi\rho_L U_0)]^{1/2}}{2} \tag{11}$$

$$X = \frac{A_c}{A_0} = \left[\frac{(D - 2h)}{D}\right]^2 \tag{12}$$

According to Rayleigh mechanism [1], assuming that the collapse of a ligament with diameter D_L will generate a droplet, then one may write [2]

$$\mathrm{SMD} = 1.89 \cdot D_L \tag{13}$$

If the semi-angle θ and the SMD estimated above are not adequate for the atomizer purposes, then a new set of dimensions must be chosen.

A water pressure-swirl atomizer with four tangential passages was designed and built according to the above described procedure. Table 1 displays the atomizer design input parameters.

Table 2 shows the results obtained in the above described calculations and the atomizer final dimensions. For the given input conditions, the combination $\theta = 39.30$ deg and SMD $= 89$ μm seems quite reasonable for combustion purposes. The dimensions were adjusted to simplify the atomizer construction. Nevertheless the above described design boundaries for the dimensionless groups were strictly respected.

III. Experimental Setup

To visualize the liquid film breakup and to measure the semi-angle (θ), a commercial Mavica–Sony MVC-FD97 camera was used. Initially, a minimum exposure time and automatic flash were used to obtain the best possible instantaneous picture. Then, a maximum exposure time and no flash were employed to obtain the spray mean outer boundaries.

Using the Photoshop® software, the pictures with longer exposure times were converted to negative form and gray scale to improve and to clarify the spray boundaries. For all cases studied here the resultant

Table 1 Atomizer design input parameters

ρ_L	1.00E + 03 kg · m^3
μ_L	1.00E − 01 kg · m^{-1} · s^{-1}
σ	7.34E − 02 kg · s^{-2}
ρ_a	1.00E + 00 kg · m^3
$\dot{m}_L$	6.00E − 03 kg · s^{-1}
ΔP_L	4.00E + 05 Pa
D_0	1.00E − 03 m

Table 2 Final results for the atomizer design

FN	3.00E − 07 m^2	L_0/D_0	1.00
X	7.30E − 01	L_p/D_p	1.60
h_0	9.31E − 05 m	D_0	1.00 mm
U_0	28.28 m · s^{-1}	D_s	3.00 mm
D_L	24.00 μm	L_s	3.00 mm
SMD	89 μm	L_0	1.00 mm
Cd [Eq. (7)]	0.27	A_p	1.20 mm^2
$A_p/(D_s \cdot D_0)$	0.40	D_p	0.60 mm
D_s/D_0	3.00	L_p	1.00 mm
L_s/D_s	1.00	θ	39.30 deg

image provides a quite well-defined cone. Then, the spray half angles were determined using the Autocad® software and the criterium to determine the cone boundary line was the line of better agreement with darker pixels, up to 3% lower than the darkest intensity.

A laser scattering system (Malvern Mastersizer X) was used to analyze the spray droplet size distribution and the SMD. When the droplets go through the helium-neon laser beam (633 nm), the circular photodiode detector plate collects the laser scattered beam in angular sectors. To obtain the droplet size distribution, the system uses the Fraunhofer diffraction theory; that is, the scattering angle is related to the droplet diameter. The scanning time is 2 ms and each measurement corresponds to 2000 scanning operations. Figure 2 shows the atomizer coupled to the laser system and the laser beam travelling through the spray.

The atomizer was assembled in a 3-D positioning system, which was needed to determine the best relative distance between the atomizer nozzle discharge orifice and the center line of the laser beam. The chosen distance was 4 cm, as this is the minimum distance for an adequate level of obscureness to be attained. For shorter distances, the obscureness level is so high for the laser beam traveling closer to the atomizer that no light signal can be detected by the photodiodes. To verify if the droplet size measurements include the occurrence of secondary breakup, the centerline of the laser beam was displaced for longer relative distances, for example, 5, 6, and 7 cm. No significant differences in SMD were detected under several atomization conditions and 4 cm was considered an adequate position of measurement.

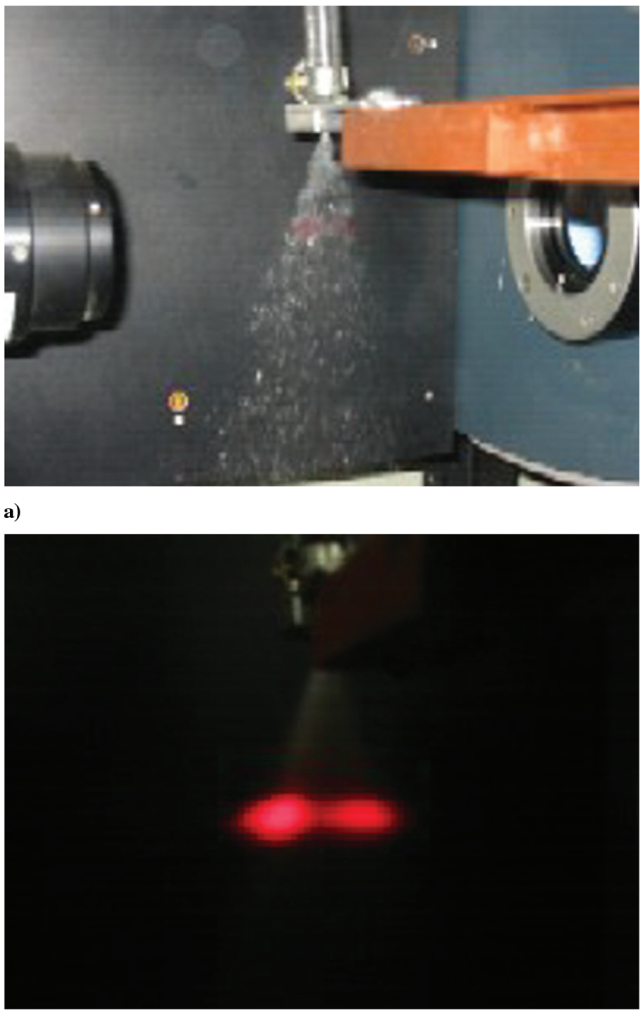

a)

b)

Fig. 2 a) Atomizer coupled to the laser system; (b) laser beam traveling through the spray.

To obtain the injector discharge coefficient, sprays under different operating pressures were discharged into a reservoir resting on a scale. The time taken to fill this reservoir with 2 kg of water was measured so that a mean liquid mass flow rate could be estimated. Then, substituting the values of the injector pressure differential and the mean mass flow rate readings in Eq. (2), the experimental discharge coefficient was estimated. The liquid flow to the atomizer is kept by nitrogen pressurization.

IV. Results

The pressure differential applied through the injector ranged from 2 to 6 atm. Under 2 atm, the liquid discharge did not generate a typical spray, but only a smooth film was formed around a hollow bubble resembling an onion; that is, of no practical interest. On the other side, 6 atm was the upper limit imposed pressure differential due to the main objective of this work which is the low injection pressure operation analysis.

Figures 3 and 4 show the liquid mass flow rate and the discharge coefficient as functions of the injector pressure differential, respectively. Figure 4 also displays the Cd used in the injector design as calculated by Carlisle [17], Risk and Lefebvre [18] and Jones [4] [Eqs. (3–5), respectively]. The experimental results consist of the mean value of 20 scans, and it can be seen that these experimental values of discharge coefficients are close to the different theoretical predictions. For instance, at the design pressure differential of 4 atm, the experimental mass flow rate and the discharge coefficient were 6.13 g/s and 0.2728, respectively, quite close to the design values of 6 g/s and 0.2700.

The experimental values of mass flow rates presented in Fig. 3 are used to predict the SMDs and the spray semi-angles.

Figure 5 shows the experimental results of SMD measurements. Each experimental value presented in Fig. 5 is the mean value of 20 scans, and repeatability was very satisfactory, with a maximum standard deviation of 0.96% for 2 atm. The rise of the atomizer pressure differential is beneficial to the SMD as expected and clearly

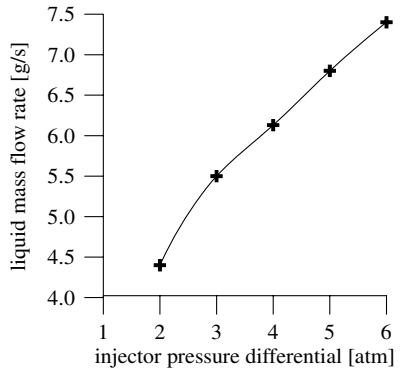

Fig. 3 Experimental liquid mass flow rate.

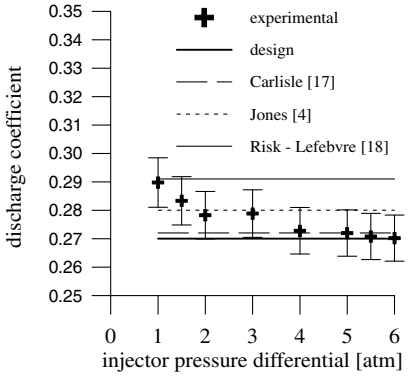

Fig. 4 Discharge coefficient as function of injector pressure differential.

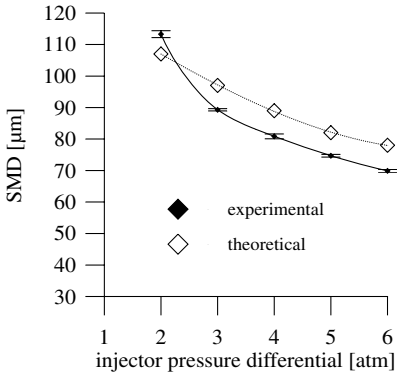

Fig. 5 Experimental and theoretical SMD as function of pressure differential.

illustrated in Fig. 5. The increase in the liquid pressure differential causes the liquid to be discharged from the nozzle at a higher velocity promoting a thinner spray. The experimental behavior of the SMD with the injector pressure differential, ΔP_L, is typical of pressure-swirl atomizers and it fully agrees with the tendency pointed out by other authors such as, for example, Wang and Lefebvre [22].

It is not enough to rely only on the SMD to verify the spray quality as one also has to make some considerations on the droplet diameter. Figure 6 presents the percentage of the total droplet volume for different pressure differentials. The values were obtained directly from data acquisition and statistical treatment software, and they were separated into three ranges of droplet diameters: from 0–19 μm, from 20–100 μm, and higher than 100 μm. Droplets smaller than 19 μm usually have low penetration and cause larger fuel concentration in regions close to the atomizer. High fuel concentration reduces the reactants mixing level, being a primary cause of increased soot formation and exhaust smoke. The second range, that is, droplets in the 20–100 μm range, is the best option for liquid fuel combustion processes due to more adequate penetration and droplet diameters sufficient for rapid vaporization in the combustion chamber. Droplets with more than 100 μm have higher vaporization time, increasing the length of mixing and burning regions.

Figure 6 also displays a well-defined droplet size distribution behavior as a function of the liquid pressure differential. The tendency is such that when the pressure increases, the percentage of droplets with a diameter smaller than 100 μm also increases. The percentage of droplets in the 0–19 μm range also increases, but not as significantly as the percentage of droplets larger than 100 μm is reduced. However, even with a liquid pressure differential of 6 atm, a situation for which the SMD seems to be quite adequate for combustion purposes, the percentage of droplets larger than 100 μm is relatively high at 42% of the total droplet volume. This can be a liability in situations requiring a high combustion rate, eventually leading to a combustion dispersion zone. Actually, this is not only a function of the droplet size distribution, but of a set of factors that influence the reactant mixing process and the combustion development itself. Therefore, atomizer performance can be fully evaluated only under actual combustion conditions.

Figure 5 also shows the prediction of SMD using the equations presented in Section II. It can be seen that the theoretical prediction agrees quite reasonably with the experimental results, nearly 10% higher than these ones, except for $\Delta P_L = 2$ atm, where the spray formation is deficient as a consequence of the low injection pressure. However, it can be considered a very good result under the design point of view, due to the simplicity of the model compared with the complex phenomena involved in liquid atomization processes.

The experimental SMD (except for the 2 atm testing) is smaller than the calculated one. The expectation was the inverse because the experimental spray angle is smaller than the calculated one, as shown

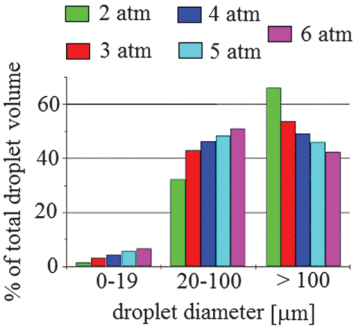

Fig. 6 Percentage of total droplet volume distribution among different pressure differentials.

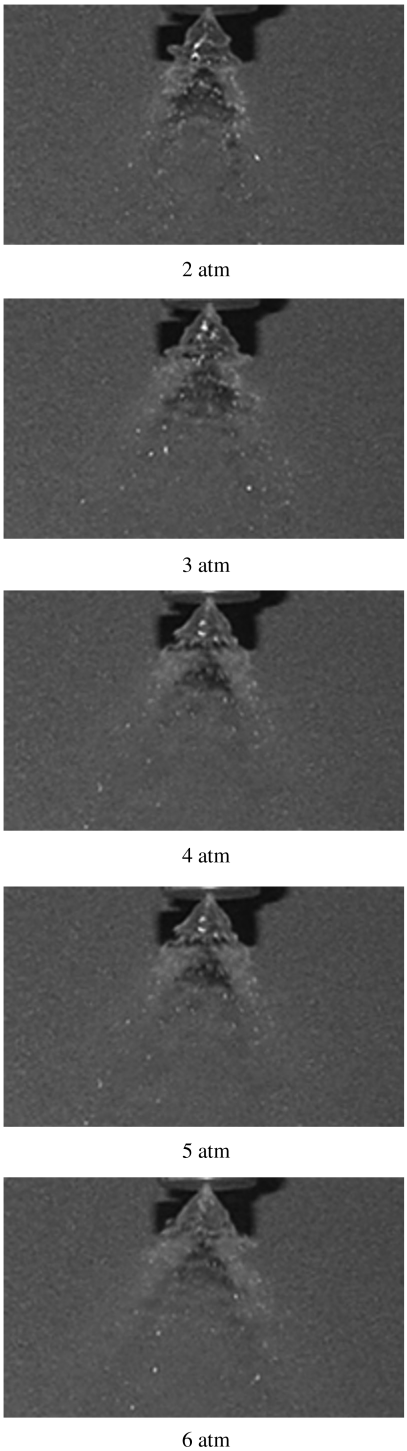

Fig. 7 Short exposition time for different injection pressures.

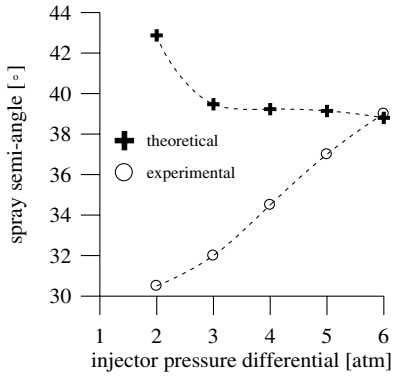

Fig. 8 Spray semi-angle as a function of the injector pressure differential.

later. However, a possible justification is that in real sprays the secondary atomization can take place, and this effect has not been included in the theoretical treatment.

The theory applied to the calculated SMD approach assumes that the atomization is in a fully developed spray stage, meaning that the curved surface forms immediately after the discharge orifice straightens to form a conical sheet; as the sheet expands its thickness diminishes, and soon it becomes unstable and disintegrates into ligaments and then into droplets generating a hollow-cone spray. However, the liquid film breakup as a function of the pressure differential can be observed in the short exposition time pictures shown in Fig. 7, where the spray is in a transition process from the "turnip" stage to the fully developed spray stage. Notice that, in all test runs, it is possible to observe that a smooth liquid film around a hollow core is formed immediately after the atomizer nozzle exit orifice, ending in a ragged edge. After that, a well-defined hollow-cone spray is established.

The consequence of the nonfully developed spray for low injection pressures is the increase of the spray semi-angle when the injection pressure also increases. However, the fully developed theory predictions showed few changes in the spray angle. Figure 8 shows the theoretical and experimental spray semi-angle as function of the injection pressures. This inconsistency is the main reason for the differences between the SMD predictions and those obtained experimentally.

The discrepancy between the design and theoretical model is based upon the fact that the model assumed a fully developed spray, whereas the actual spray regime is not fully developed. In the fully developed spray theory the spray semi-angle did not change with injection pressure, whereas the experimental semi-angles changed considerably with variations in injection pressure. This behavior was observed by Reddy and Mishra [7] who also experimentally investigated the spray behavior of pressure-swirl atomizer low pressure operation, up to nearly 5 atm. At this transition regime, they observed that by increasing the applied pressure the surface tension is gradually overcome as a consequence of the centrifugal force increase, the conical sheet collapses upon emerging from the atomizer, and the spray-cone angle increases monotonically with the injection pressure as observed in the present paper.

Another result observed in this work that agrees with the work of Reddy and Mishra [7] is the SMD measurement. Initially, the droplet size decreases rapidly with increasing pressure, but the influence of the injection pressure gradually decreases at higher pressure injection values. This is due to the fact that at low injection pressures, the conical sheet collapses and is characterized by a large degree of coalescence. With increasing pressure, the liquid sheet diverges and the sheet breakup is controlled mostly by the surface waves due to increased aerodynamic drag leading to finer atomization patterns.

V. Conclusions

This work describes a design procedure based in previous works concerning pressure-swirl atomizer. However, for this case, the procedure is used to design a low pressure injection atomizer, whose practical interest resides in the lower power stages of liquid-fueled gas turbine operations.

The SMD and the spray-cone angle are evaluated during the calculation of the atomizer dimensions. The liquid mass flow rate, the discharge coefficient, the spray semi-angle, the SMD, and the droplet size distribution were obtained experimentally to evaluate the spray and to be compared with the theoretical results obtained from the design methodology.

For all investigated pressure differentials, the spray visualization showed the presence of a smooth liquid film before the droplet formation, characterizing a transition from the turnip stage into the fully developed spray stage. The consequence of the nonfully developed spray in the range of injection pressures studied here, that is, low pressures, is the strong dependence of the semi-angle on the pressure injection. The methodology used to predict the semi-angle is based on a fully developed spray, and the semi-angle does not depend on the pressure injection, but on the discharge coefficient. This inconsistency is the main reason for the difference between the experimental semi-angle observed value and its value obtained from theoretical evaluation. It is important for pressure-swirl atomizer designers to know that the real tendency in low pressure injection cases is to obtain smaller semi-angles than the predicted ones.

As the semi-angle has influence in the SMD prediction [as it can be seen due to the presence of the $\cos(\theta)$ in Eq. (9) used for the ligament diameter calculation], some differences were observed in comparison to the experimental results. However, it can be seen that the theoretical prediction is never higher than 10% of the experimental results, (except for $\Delta P_L \leq 2$ atm, when the spray formation becomes completely deficient due to the low injection pressure, as already mentioned). Taking into account the simplicity of the suggested analytical model for the SMD prediction and the fact that atomization is a very complex process, a maximum 10% departure from experimental results is quite reasonable for design purposes.

A single injector was evaluated here designed for dimensions, mass flow rates, and injection pressures typical for gas turbine pilot nozzles under low power operation modes and the results are qualitatively acceptable for pressure-swirl atomizers designed specifically for this situation of injection. The results should not be generalized, especially for injectors designed for higher pressures, higher mass flow rates, and large scale nozzles.

Acknowledgments

Part of this work (Bastos-Netto and Lacava) was sponsored by the Brazilian National Research Council (CNPq) under Grants No. 352289/1992-2 and No. 302505/2004-0. The tests were carried out at the Professor Feng Aeronautical Laboratory, Aeronautical Technology Institute.

References

[1] Lefebvre, A. H., *Atomization and Sprays*, Hemisphere, New York, 1989.

[2] Couto, H. S., Carvalho, J. A., Jr., and Bastos-Netto, D., "Theoretical Formulation for Sauter Mean Diameter of Pressure-Swirl Atomizers," *Journal of Propulsion and Power*, Vol. 13, No. 5, 1997, pp. 691–696. doi:10.2514/2.5221

[3] Dombrowski, N., and Johns, W. R., "The Aerodynamic Instability Disintegration of Viscous Liquid Sheets," *Chemical Engineering Science*, Vol. 18, No. 2, 1963, pp. 203–214.

[4] Jones, A. R., "Design Optimization of a Large Pressure-Jet Atomizer for Power Plant," *Proceedings of the 2nd International Conference on Liquid Atomization and Spray Systems*, Hemisphere, New York, 1982, pp. 181–185.

[5] Lefebvre, A. H., *Gas Turbine Combustion*, Hemisphere, New York, 1983.

[6] Marchione, T., Allouis, C., Amoresano, A., and Beretta, F., "Experimental Investigation of a Pressure Swirl Atomizer Spray," *Journal of Propulsion and Power*, Vol. 23, No. 5, Sept.–Oct. 2007, pp. 1096–1101. doi:10.2514/1.28513

[7] Reddy, K. Y., and Mishra, D. P., "Studies on Spray Behavior of a Pressure Swirl Atomizer in Transition Regime," *Journal of Propulsion and Power*, Vol. 24, No. 1, Jan.–Feb. 2008, pp. 74–80. doi:10.2514/1.31156

[8] Santolaya, J. L., Aísa, L. A., Calvo, E., García, I., and Cerecedo, L. M., "Experimental Study of Near-Field Flow Structure in Hollow Cone Pressure Swirl Sprays," *Journal of Propulsion and Power*, Vol. 23, No. 2, March–April 2007, pp. 382–389. doi:10.2514/1.20713

[9] Kim, D., Im, J.-H., Koh, H., and Yoon, Y., "Effect of Ambient Gas Density on Spray Characteristics of Swirling Liquid Sheets," *Journal of Propulsion and Power*, Vol. 23, No. 3, May–June 2007, pp. 603–611. doi:10.2514/1.20161

[10] Paula Souza, J. R., "Experimental Analysis of a Pressure-Swirl Bi-Propellant Atomizer for Liquid Propellant Rocket Engines," M.Sc., Dissertation, Instituto Tecnológico de Aeronáutica, São José dos Campos, Brazil, 2001, also "Estudo de um Injetor Centrífugo Bipropelente utilizado em Motor Foguete a Propelente Líquido" (in Portuguese).

[11] Bazarov, V. G., and Yang, V., "Liquid-Propellant Rocket Engine Injector Dynamics," *Journal of Propulsion and Power*, Vol. 14, No. 5, 1998, pp. 797–806. doi:10.2514/2.5343

[12] Kim, D., Han, P., Im, J.-H., Yoon, Y., and Bazarov, V. G., "Effect of Recess on the Spray Characteristics of Liquid-Liquid Swirl Coaxial Injectors," *Journal of Propulsion and Power*, Vol. 23, No. 6, Nov.–Dec. 2007, pp. 1194–1203. doi:10.2514/1.30450

[13] Ramezani, A. R., and Ghafourian, A., "Spray Angle Variation of Liquid-Liquid Swirl Coaxial Injectors," AIAA Paper 2005-3747, 10–13 July 2005.

[14] Xue, J., Jog, M. A., Jeng, S. M., Steinthorsson, E., and Benjamin, M. A., "Effect of Geometric Parameters on Simplex Atomizer Performance," *AIAA Journal*, Vol. 42, No. 12, 2004, pp. 2408–2415. doi:10.2514/1.2983

[15] Elkotb, M. M., Rafat, N. M., and Hanna, M. A., "The Influence of Swirl Atomizer Geometry on the Atomization Performance," *Proceedings of the 1st International Conference on Liquid Atomization and Spray Systems*, Hemisphere, New York, 1978, pp. 109–115.

[16] Tipler, W., and Wilson, A. W., "Combustion in Gas Turbines," *Proceedings of the Congress International des Machines a Combustion (CIMAC)*, Hemisphere, New York, 1959, pp. 897–927.

[17] Carlisle, D. R., "Communication on the Performance of a Type of Swirl Atomizer," edited by A. Radcliffe, *Proceedings of the Institution of Mechanical Engineers*, Vol. 169, No. 1, 1955, p. 101.

[18] Risk, N. K., and Lefebvre, A. H., "Internal Flow Characteristics of Simplex Swirl Atomizers," *Journal of Propulsion and Power*, Vol. 1, No. 3, 1985, pp. 193–199. doi:10.2514/3.22780

[19] Jeng, S. M., Jog, M. A., and Benjamin, M. A., "Computational and Experimental Study of Liquid Sheet Emanating from Simplex Fuel Nozzle," *AIAA Journal*, Vol. 36, No. 2, 1998, pp. 201–207. doi:10.2514/2.7502

[20] Sakman, A. T., Jog, M. A., Jeng ,S. M., and Benjamin, M. A., "Parametric Study of Simplex Fuel Nozzle Internal Flow and Performance," *AIAA Journal*, Vol. 38, No. 7, 2000, pp. 1214–1218. doi:10.2514/2.1090

[21] Giffen, E., and Muraszew, A., *Atomization of Liquid Fuels*, Chapman & Hall, London, 1953.

[22] Wang, X. F., and Lefebvre, A. H., "Mean Drop Sizes From Pressure Swirl Nozzles," *Journal of Propulsion and Power*, Vol. 3, No. 1, 1987, pp. 11–18. doi:10.2514/3.22946

D. Talley
Associate Editor